Scientific Research Publishing

American Journal of Analytical Chemistry, 2019, 10, 459-475
https://www.scirp.org/journal/ajac
ISSN Online: 2156-8278
ISSN Print: 2156-8251

Electron Transfer of *Shewanella oneidensis* MR-1 at Clay-Modified ITO Electrode

Reem Alshehri[1,2*], Alanah Fitch[1]

[1]Department of Chemistry and Biochemistry, Loyola University Chicago, Chicago, USA
[2]Department of Chemistry, Taibah University, Al-Ula, KSA
Email: *ralshehri1@luc.edu

How to cite this paper: Alshehri, R. and Fitch, A. (2019) Electron Transfer of *Shewanella oneidensis* MR-1 at Clay-Modified ITO Electrode. *American Journal of Analytical Chemistry*, **10**, 459-475.
https://doi.org/10.4236/ajac.2019.1010033

Received: September 16, 2019
Accepted: October 9, 2019
Published: October 12, 2019

Abstract

The electrode material is an important aspect for the efficiency and costs in the microbial fuel cells (MFCs). Enhancing of current production and bacteria attachment to the electrode are essential goals for developing the performance of MFCs. In this study, the role of the structural iron present in clays in enhancing the electron transfer of *Shewanella oneidensis* MR-1 was investigated. Two types of clay containing different amounts of iron situated in the octahedral sites were used to modify ITO (indium tin oxide) electrodes, namely nontronite NAu-1, and montmorillonite (Wyoming) SWy-1. Synthetic montmorillonite SYn-1 which is iron-free clay was used for comparison. The interaction between the bacterial cells and the clays was studied by potential-step chronoamperometry, cyclic voltammetry, confocal microscopy, and scanning electron microscopy (SEM). The obtained results showed that the current densities generated upon ITO electrode modification using the NAu-1 and SWy-1 iron-containing clays were 19 and 3 times higher than that produced using the bare ITO electrode. No current density was obtained when utilizing the synthetic montmorillonite SYn-1 clay. SEM and confocal microscopy observations confirmed the increased coverage percentage of the bacterial cells attached to the clay-modified electrodes compared to the bare ITO.

Keywords

Shewanella oneidensis MR-1, Clay, Modified ITO Electrode, Microbial Fuel Cell

1. Introduction

Electron transfer from organic matter such as glucose or lactate is an important

process in microbial fuel cells (MFCs) where bacteria act as catalyst. More specifically, MFCs are a form of a bioreactor that generates electricity from chemical energy using electrodes. Wastewater treatment, power generation, and biosensors are the most widely used applications for MFCs [1] [2] [3] [4]. *Shewanella oneidensis* MR-1 is a commonly used bacterium in MFCs since it contains cytochromes in its outermost protective membrane, and these cytochromes transport electrons to nearby electron acceptors. Under anaerobic conditions, the *Shewanella oneidensis* bacterium reduces the terminal electron acceptors such as Mn(III), Fe(III), nitrate, fumarate, thiosulfate, trimethylamine N-oxide, dimethyl sulfoxide, sulfite, and elemental sulfur [5].

To date, various strategies have been established to enhance the extracellular electron transfer and energy output capability of MFCs, with the majority being aimed at anode modification [6], substrate sources [7], redox mediators [8], and bioreactor configurations [9]. The anode has a significant impact on the electricity generation performance of MFCs because it is in direct contact with the microorganisms. Lately, the applications of different modified electrodes have been studied such as, the (CNTs/PAH) ITO electrode [10], the $(Fe_2O_3/CS)_4$ ITO electrode [11], and the $(PAH/GE)_2$ ITO electrode [12].

Clay minerals are abundantly found in soils, rocks, and sediments, and find application in various fields including pharmaceuticals, pottery, animal feed, wastewater treatment, oil adsorbents, and antibacterial agents [13] [14]. Clays are layered materials that consist of tetrahedral silicates (Si-O) and/or octahedral aluminates (Al-O, Al-OH). Clays may contain one silicate and one aluminate sheet, which is known as a 1:1 layer; this type of clay is known as kaolinite. In addition, clays can contain one octahedral sheet sandwiched between two tetrahedral sheets, such as montmorillonite, and nontronite [15]. Clay layers also contain Al^{3+}, Si^{4+}, Mg^{2+}, and Fe^{3+} in their octahedral and tetrahedral sheets, and many exchangeable cations exist between the clay layers, such as Na^+, Ca^{2+}, and K^+, which balance the negative charges of the clay layers. **Table 1** shows the compositions and formula of the three clays employed herein.

In recent decades, clay-modified electrodes (CME) have attracted the attention of electrochemists worldwide, and as such, they are found in a variety of applications including sensors [18] [19] [20]. Indeed, the combination of clays with electrodes provides the desired sensitivity, durability, selectivity, and speed of sensors. Moreover, it should be noted that the cost of preparing clay-modified sensors is significantly less than for the preparation of other types of modified sensors [21]. In the case of CMEs, electron transfer occurs through channels by

Table 1. Compositions and formula of the clays employed herein.

Clay	Name	Formula [16]	$\%Fe_2O_3$ [16]	CEC meq/100g
NAu-1	Nontronite	$M+(1.0)[Al_{0.58}Fe_{3.38}Mg_{0.05}][Si_{7.00}Al_{1.00}]O_{20}(OH)_4$	34.19	74.7 [17]
SWy-1	Montmorillonite (Wyoming)	$M+(0.49)[Al_{3.01}Fe(III)_{0.41}Mn_{0.01}Mg_{0.54}Ti_{0.02}][Si_{7.98}Al_{0.02}]O_{20}(OH)_4$	3.35	76.4 [16]
SYn-1	Synthetic montmorillonite	$M+(0.22)[Al_{3.99}Fe(III)trMn_{tr}Ti_{tr}][Si_{6.50}Al_{1.50}]O_{20}(OH)_4$	0.02	70.0 [16]

the physical diffusion of mediators within the clay film [22] [23]. Furthermore, electrons can hop through redox-active cations (e.g., iron) within the clay crystals to impart charge transfer in a CME [24] [25]. The use of clay is also considered a green initiative, and so these materials are often preferred instead of other, often toxic, chemicals. Moreover, the waste produced through the modification of electrodes using clay is negligible, and so fewer protocols and permissions are required compared to when other materials or chemicals are employed.

Interestingly, it has been reported that the presence of iron in the crystal structures of smectite clays highly impacts their physical and chemical properties. It has been proposed that these iron atoms are involved in the electron transfer process thereby influencing the response of clay-modified electrodes. For example, iron involvement in the electron transfer of cytochrome c (Cyt-c) at a montmorillonite CME was reported by Scheller [26], while Charade and coworkers found that the structural iron present in clays promotes the direct electron transfer of hemoglobin. They examined different types of clays, including nontronite, synthetic montmorillonite, saponite, and synthetic montmorillonite containing non-iron impurities, they found that nontronite, which contains the highest amount of structural iron, significantly enhanced the direct electron transfer of hemoglobin [27]. In addition, Oyama and Anson concluded that the structural iron present in montmorillonite clay mediates the reduction of hydrogen peroxide [28], while Koffi reported the use of clay-modified carbon paste electrodes to determine the presence of bacteria in water and blood samples [29]. However, the possible role of structural iron in the electron transfer process of metal-reducing bacteria such as *Shewanella oneidensis* MR-1 has yet to be investigated using CMEs.

Thus, we herein report our investigation into the effect of the structural iron present in clay to enhance the direct electron transfer of *Shewanella oneidensis* MR-1. As clay works as an alternative surface to attract bacteria and facilitate electron transfer through the iron present in the octahedral sheet, we employ two ferruginous clays containing different amounts of iron situated in their octahedral sheets, in addition to one iron-free synthetic montmorillonite for comparison.

2. Materials and Methods

2.1. Materials

Shewanella oneidensis MR-1 microbes were purchased from The Global Bioresource Center (ATCC). The Wyoming montmorillonite (SWy-1), nontronite (NAu-1), synthetic montmorillonite (SYn-1) clays were obtained from the Source Clay Minerals Repository (Purdue University, East Lafayette, Ind., Department of Agronomy). Tryptic soy broth (TSB), NaCl, KCl, and $K_3[Fe(CN)_6]^{3-}$ were purchased from Sigma Aldrich.

2.2. Preparation of the Clay-Modified ITO Electrodes

The desired clay suspensions were prepared by stirring the corresponding clay

in deionized water (500 mL) to give a total clay concentration of 5 g/L for each case. The ITO (indium tin oxide) glass slides (Thin Film Devices, Inc.) were washed, rinsed, dried, and wiped with 70% isopropyl alcohol, re-dried, and allowed to equilibrate with air. Portions of the clay gel (100, 300, 500, or 800 μL) were then smeared uniformly on the ITO slide using a micropipette and left to air-dry overnight. The film thicknesses were measured by SEM. Water contact angles were determined using a Veho discovery camera and MicroCapture software. Each measurement was carried out in duplicate and the data were averaged.

2.3. Potassium Ferricyanide Experiments

Solutions of NaCl and KCl were prepared in distilled water at concentrations of 0.05, 0.1, 0.3, 0.5, 0.7, 0.9, and 1.2 M. Subsequently, 3 mM solutions of $K_3[Fe(CN)_6]^{3-}$ were prepared in different concentrations of the NaCl and KCl salt solutions, and all solutions were subjected to N_2 purging for 10 min prior to use in the electrochemical cell. Each clay film was soaked for 10 min in the desired salt electrolyte solution and then exposed to the $K_3[Fe(CN)_6]^{3-}$ solution. The response of the CMEs in the presence of different cation electrolytes and $K_3[Fe(CN)_6]^{3-}$ was monitored by cyclic voltammetry with scanning between 0.8 and −0.4 V vs. Ag/AgCl at a scan rate of 10 mV/s.

2.4. Microbial Culture

Shewanella oneidensis MR-1 from a −80˚C freezer stock was inoculated into TSB medium (100 mL) and incubated at 30˚C for 12 h anaerobically. After this time, the optical density was measured at 650 nm using a VWR UV6300PC double-beam spectrophotometer. The optical density of the culture solution before harvest in the electrochemical cell was 0.3 for all experimental conditions examined. The OD_{650} of the original culture solution and the culture solution recovered from the electrochemical cell were also measured post-experiment. Finally, the resulting cell suspension was centrifuged at 5000 rpm for 10 min to produce cell pellets to which fresh and N_2-purged TSB medium (100 mL) was added. Three triplicate samples were run on the electrochemical cell on the same day.

2.5. The Electrochemical Cell

The electrochemical cell employed for the electrochemical study consisted of a single-chamber with three-electrodes. A tin-doped In_2O_3 (ITO) substrate on glass slides (surface area of 4.5 cm^2), which had been modified by the clay film, was used as the working electrode (WE). Ag/AgCl (NaCl saturated) and a platinum wire were used as the reference and counter electrodes, respectively. The cell was positioned such that the ITO (WE) was vertical with the solution pumped from the side and exiting at the top. The positioning was chosen to minimize the gravitational deposition of bacteria on the slide. The clay film on the

electrode was soaked for 10 min in N_2-purged TSB prior to use in the electrochemical experiment. Immediately afterwards, the bacterial culture solution (11 mL) was pumped into the electrochemical cell. For each condition, the current was measured for 2 h at a potential of +0.2 V. Subsequently, cyclic voltammetry was carried out with initial and final potentials of +0.2 V, a switching potential of −0.5 V, and a scan rate of 5 mV/s. Epsilon EC was used for the electrochemical experiments.

2.6. Confocal Microscopy

After completion of the electrochemical experiment, the WE was removed from the cell, and left to dry in a vertical position to reduce the pooling and drying of unattached microbes. An Olympus Compound Microscope BH2-RFCA and ImageJ software were used to monitor the changes in the bacterial cell coverage percentage over the clay-modified ITO electrodes.

2.7. Scanning Electron Microscopy (SEM)

The *Shewanella oneidensis* MR-1 microbes attached on the modified electrodes were imaged using SEM (HITACHI, SU3500). After the electrochemical experiment, the clay-modified ITO was fixed with a 2.5% glutaraldehyde solution for 2 h, rinsed three times in phosphate buffer (pH 7.0, 50 mM), dehydrated using a series of ethanol solutions (60%, 70%, 80%, 90%, 95%, and 100%), and then air-dried [30].

3. Results and Discussion

3.1. Characterization of the Clay-Modified ITO Electrodes

3.1.1. Particle Size, Clay Texture, and Film Thickness

The particle size of a clay is known to affect both the absorption [31] and diffusion [32] through the clay layers. As such, the particle size distributions of the different clays employed herein were determined, as outlined in **Figure 1** (top). As indicated, NAu-1 has a particle size of <1 μm, SYn-1 has a particle size of <5 μm, and SWy-1 exhibited a particle size distribution of 0.5 - 50 μm.

Indeed, the particle size analyses were found to be consistent with the clay surface textures shown in **Figure 1** (bottom), where NAu-1 and SYn-1 appear to have smooth and flat surfaces, while SWy-1 shows roughness and the presence of bridging surfaces. As outlined in **Table 1**, the cation exchange capacities (CECs) of these clays are similar (*i.e.*, 74.7, 76.4 and 70.0 meq/100g). The film thicknesses were then determined by SEM through measurement of the thickness at three different points and taking an average; film thicknesses ranging from 5 to 16 μm were recorded. **Figure 2** shows the thinnest area of each film on the ITO electrode, and it is apparent that NAu-1 and SYn-1 formed compact films, while SWy-1 gave an expanded film. This observation is relevant since more compact the film is, the more difficult it is for any species to diffuse through the film. The thicker film formed in the case of SWy-1 (7 μm) was likely

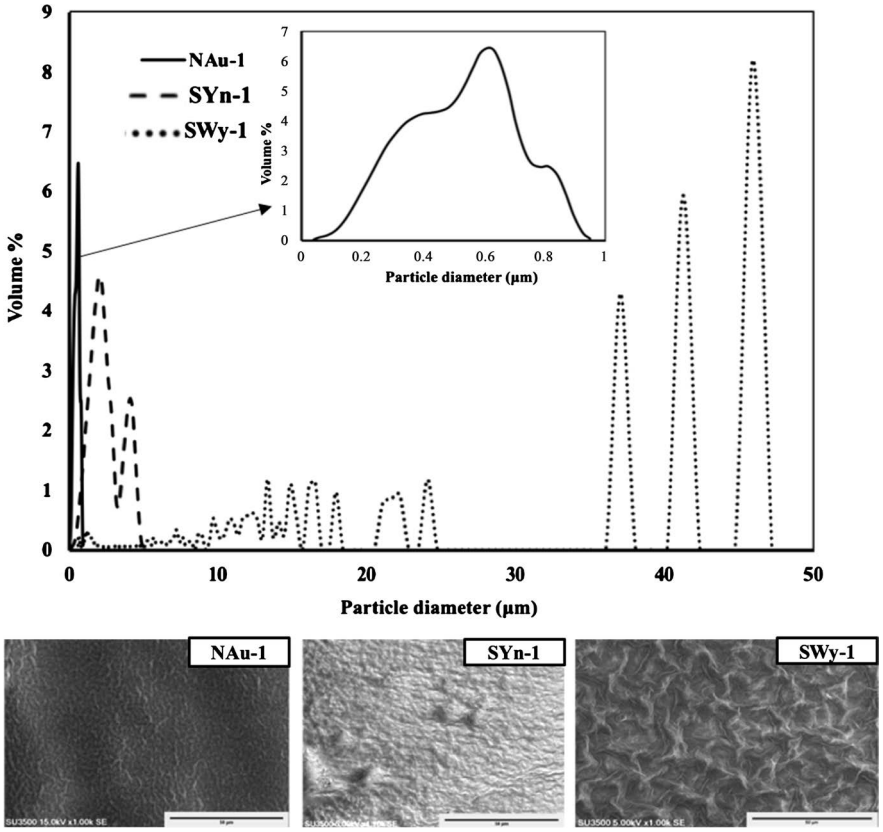

Figure 1. Top: particle size distribution of nontronite NAu-1 (solid line), synthetic montmorillonite SYn-1 (dashed line), and Wyoming SWy-1 (dotted line). Bottom: SEM images of the three clay-modified electrodes.

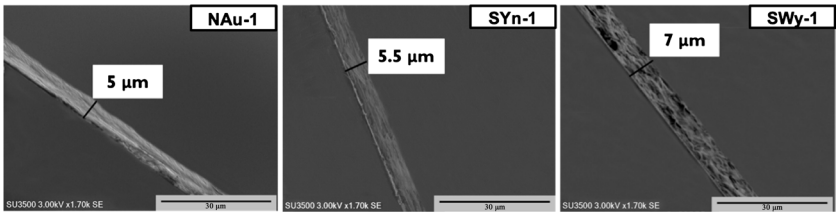

Figure 2. Thicknesses of the clay films on the ITO electrodes. The thinnest regions are shown.

due to the larger particle size. The thickest film used in this study was 16 μm which is much smaller than the thickness used in [33], the iron-containing clays have an excellent electrocatalytic activity.

3.1.2. Electrochemical Behavior of $Fe(CN)_6$ in the Clay Films: Determination of the Film Porosity and Coverage

Clay interlayers expand when exposed to water since the hydrated exchangeable cations force the clay layers apart. Thus, the coverage and porosity of each expanded film can be examined using a $[Fe(CN)_6]^{3-}$ solution since this electrochemically active ion is negatively charged, thereby forcing it to move through the larger pores of the film [34]. The currents measured were recorded as the ratio of the current at the clay-modified ITO electrode to that at the bare ITO

electrode. Different ratios reflect differences in the interlayer spacing through the clay film [35].

Figure 3 shows the relationship between the ratio of the reduction current and the NaCl concentrations for the thinnest and thickest clay film areas. As expected, the highest ratio was obtained for the thinner areas (dashed line), indicating that the clay covered less of the surface. More specifically, at a low NaCl concentration, the corresponding ratios were 0.94, 0.89, and 0.87 for montmorillonite SWy-1, SYn-1, and NAu-1, respectively. Upon increasing the NaCl concentration, the ratio decreased to 0.54, 0.50, and 0.46 for montmorillonite SWy-1, SYn-1, and NAu-1, respectively. In contrast, a lower ratio was found for the thicker film areas (solid line), which is consistent with a greater surface coverage. More specifically, at the lowest NaCl concentration, these ratios were 0.68, 0.61, and 0.56 for montmorillonite SWy-1, SYn-1, and NAu-1, respectively, while upon increasing the NaCl concertation to 1.2 M, the ratios decreased to 0.22, 0.14, and 0.10, respectively.

The above observations can be accounted for by the fact that at low salt concentrations, the interlayer expands, causing an increase in the pore space, and allowing for increased diffusion of the probe ion. Upon increasing the salt concentration, the interlayer is compacted, thereby decreasing the available pore space, and reducing the amount of diffusion. Since the dehydration of Na^+ cations requires a large amount of energy, they can enter the interlayer in their hydrated form, thereby forcing apart the clay layers. In contrast, soaking the clay in a KCl solution creates compact layers since the K^+ cations are easily dehydrated and have a low hydration energy compared to Na^+ [35]. KCl-soaked clays

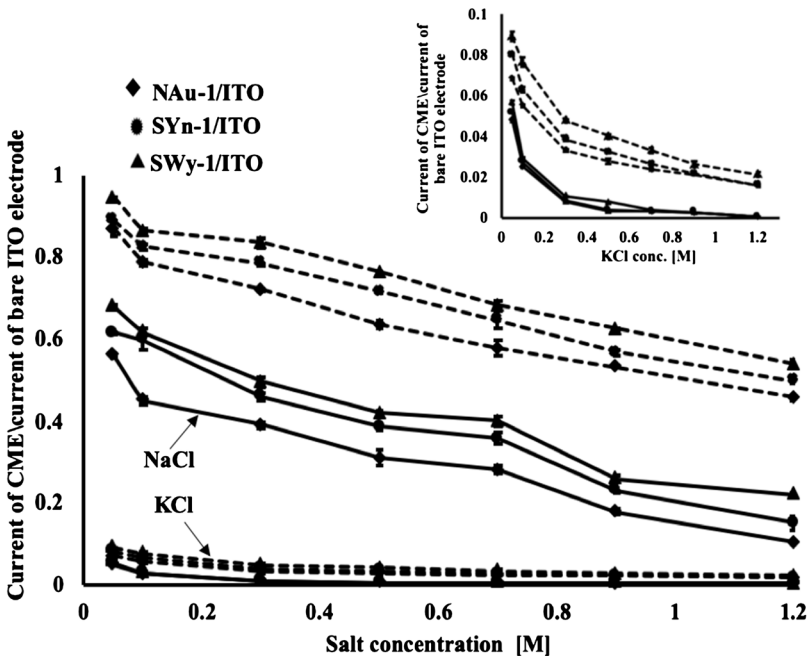

Figure 3. Ratio currents for the three clays as a function of the electrolyte concentration and type, (dashed lines) represents the thinnest area and (solid lines) represents the thickest area for each clay.

should therefore exhibit reduced porosities. Considering that an R value of ≤0.04 is considered to represent complete coverage of the surface [36], the R values for the thinnest and thickest parts of the films were determined in the presence of 1.2 M KCl, and were found to be <0.02 (see **Figure 3**), thereby indicating that the clay completely covered the ITO electrode for both extremes of thicknesses.

All clays, regardless of the particle size (NAu-1 < SYn-1 < SWy-1), exhibited a decreasing porosity upon increasing the NaCl concentration and in the presence of KCl. However, we note that the porosity is also affected by the particle size, and the particle size findings shown in **Figure 1** combined with the probe ion experiments presented in **Figure 3** confirmed that as the particle size decreased, the porosity also reduced, and so diffusion decreased.

3.2. Clay-Modified ITO Electrode with Shewanella Oneidensis MR-1

3.2.1. Chronoamperometry

Figure 4(a) shows the current density as a function of time during the loading process at +0.2 V, where the thickest regions of the clay films were employed. As

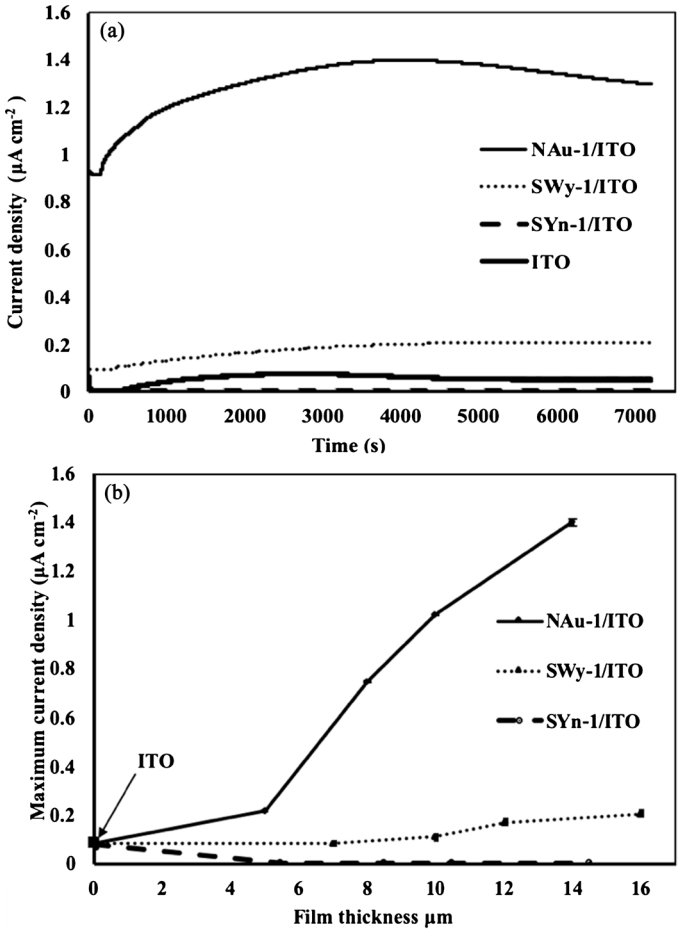

Figure 4. (a) Current density generated as a function of time for *Shewanella oneidensis MR*-1 on the clay-modified ITO electrodes at +0.2 V for the thickest film regions; (b) Variation in the current densities with a range of film thicknesses.

indicated, the maximum current density obtained by the NAu-1/ITO electrode was (1.40 ± 0.0015 μA·cm^{-2}), which is approximately 19 times higher than that of the bare ITO electrode (0.07 ± 0.0013 μA·cm^{-2}), while the maximum current density obtained for the SWy-1/ITO electrode was (0.26 ± 0.0014 μA·cm^{-2}), which is approximately 3 times higher than that of the bare ITO electrode. No current was obtained when using the SYn-1/ITO electrode.

As presented previously in **Figure 3**, an increase in the film thickness results in a reduced porosity, thereby indicating that thick clay films should inhibit charge transfer from the bacteria to the underlying clay surface. Indeed, such behavior was observed for SYn-1, which exhibited inhibited charge transfer. However, contrasting results were observed for the iron-containing clays, *i.e.*, NAu-1 and SWy-1 (**Figure 4(b)**), where the maximum current density was found to increase upon increasing the clay film thickness. This suggests that the increase in current density may be caused by iron-mediated charge transfer. We also note that the increase in the maximum current density with film thickness was significantly higher for the NAu-1/ITO electrode than the SWy-1/ITO electrode.

As outlined in **Table 1**, since NAu-1 is an iron-rich clay, it contains greater quantities of Fe^{3+} in its octahedral sheet than the SWy-1 clay; SYn-1 does not contain iron and does not produce any current, thereby providing further evidence that electron transfer occurs through the Fe^{3+} present in the clay. It should be noted that the majority of the structural iron in clay is ferric iron that can be reduced biologically by metal-reducing bacteria [37] [38] [39] [40]. The structural Fe^{3+} present in the clay acts as an electron acceptor, while the organic matter present in the growth media serves as an electron donor. In the bio-reduction process, metal-reducing bacteria attach themselves to the clay surface [13], and microorganisms reduce the structural Fe^{3+} in the clay to Fe^{2+} [37] [38] [41]. which can be re-oxidized by pollutants such as chlorinated solvents, nitroaromatic explosives [42] [43] [44], and metals such as U, Tc, and Cr [45] [46] [47]. At least 90% of the structural Fe^{2+} can be re-oxidized to Fe^{3+} [48] [49]. Also of importance is the fact that *Shewanella oneidensis* MR-1 contains cytochromes in the outer membrane [50] [51] [52] [53], and an attractive force has been detected between *Shewanella oneidensis* whole cells and the hematite surfaces [54]. Moreover, specific bonding has been detected between MtrC and hematite surfaces [55], and direct attraction exists between OM C-type cytochromes and Fe^{3+} and the localization of the cytochromes on the cell surface. MtrC is therefore localized at the interface between the *Shewanella oneidensis* cells and hematite during Fe^{3+} reduction [56] [57].

However, an alternative hypothesis may be proposed. As the bacterial cell wall is partially negatively charged and partially lipid in character, it could be anticipated that bacteria are more greatly attached to surfaces exhibiting both characteristics. Upon considering the hydrophilicity, which can be measured using the contact angle, θ_c, the hydrophilicity of the bare ITO electrode was found to be low (*i.e.*, a large θ_c ~70.0˚). Interestingly, the contact angles for the clays varied

in an order that was inconsistent with the obtained currents densities presented in Figure 4. More specifically, the current densities decreased in the order NAu-1/ITO > SWy-1/ITO > SYn-1/ITO, while the contact angles decreased in the order SWy-1/ITO (~30.0˚) > SYn-1/ITO (~20.0˚) > NAu-1/ITO (~15˚), thereby suggesting that the iron content is a greater driving force than the hydrophilicity in determining the current density.

3.2.2. Cyclic Voltammetry (CV) and Electric Charge (Q) Measurements

After chronoamperometry at +0.2 V for 2 h, the cyclic voltammograms of the clay-modified ITO electrodes were recorded, where Figure 5(a) shows the voltammograms for NAu-1/ITO, SWy-1/ITO, SYn-1/ITO, and the bare ITO electrode. Redox peaks with a midpoint potential of −0.19 V were found to be consistent with that of the outer membrane Cyts-c which exhibits a wide potential range of 0.13 to −0.27 V [58] [59].

The cyclic voltammetry results are consistent with those of the chronoamperometry experiments presented in Figure 4, where the NAu-1/ITO electrode exhibited the highest reduction peak current density (3.84 ± 0.15 μA·cm^{-2}), and the SWy-1/ITO electrode gave a reduction peak current density of 2.26 ± 0.34 μA·cm^{-2}.

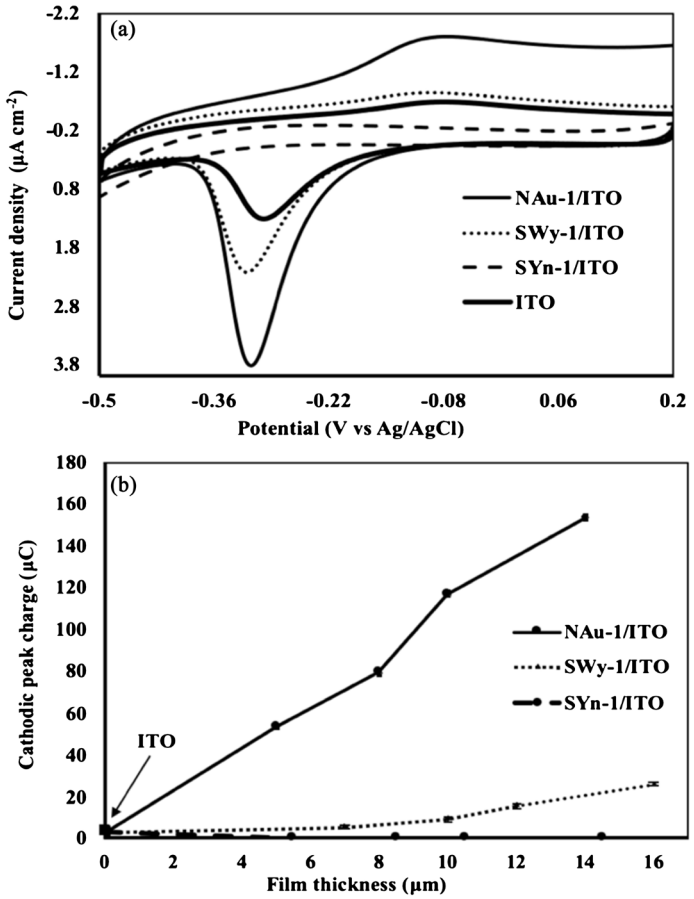

Figure 5. (a) Cyclic voltammograms (CV) of the clay-modified ITO electrode after 2 h of chronoamperometry at a scan rate of 5 mV/S for the thickest film of each clay; (b) The cathodic peak charge (Q) versus the film thickness for each clay-modified electrode.

For comparison, we note that the reduction peak current density of the bare ITO was 1.33 ± 0.06 μA·cm^{-2}, and no reduction peak current density was obtained with SYn-1/ITO.

In addition, Figure 5(b) shows the total quantity of electric charge (Q) versus the film thickness for each clay type, where Q was calculated by integrating the area under the reduction peak in the cyclic voltammogram using the following equation [30]:

$$Q = \int_0^t I\mathrm{d}t \tag{1}$$

where I is the current and t is the working time. The black square in Figure 5(b) represents the Q value obtained using the bare ITO electrode, which is equal to 2.95 ± 0.4 μC. The Q values obtained for the thickest NAu-1/ITO and SWy-1/ITO films were 153.58 ± 1.2 and 25.84 ± 0.9 μC, respectively. No Q value was obtained for the iron-free SYn-1/ITO clay.

3.2.3. SEM Imaging and Determination of the Area Coverage Percentage by Confocal Microscopy

Figure 6 shows the SEM images obtained for the attached bacterial cells on the clay-modified ITO electrode for the thickest film of each clay. As indicated, the bare ITO (A) and SYn-1/ITO (B) electrodes exhibited approximately 30% and 29% bacterial coverage, respectively, while the SWy-1/ITO (C) electrode exhibited a greater coverage of ~43%, and the iron rich clay NAu-1/ITO electrode demonstrated the highest bacterial cell coverage of ~86%.

Interestingly, as outlined in Figure 7, a relationship was found between the

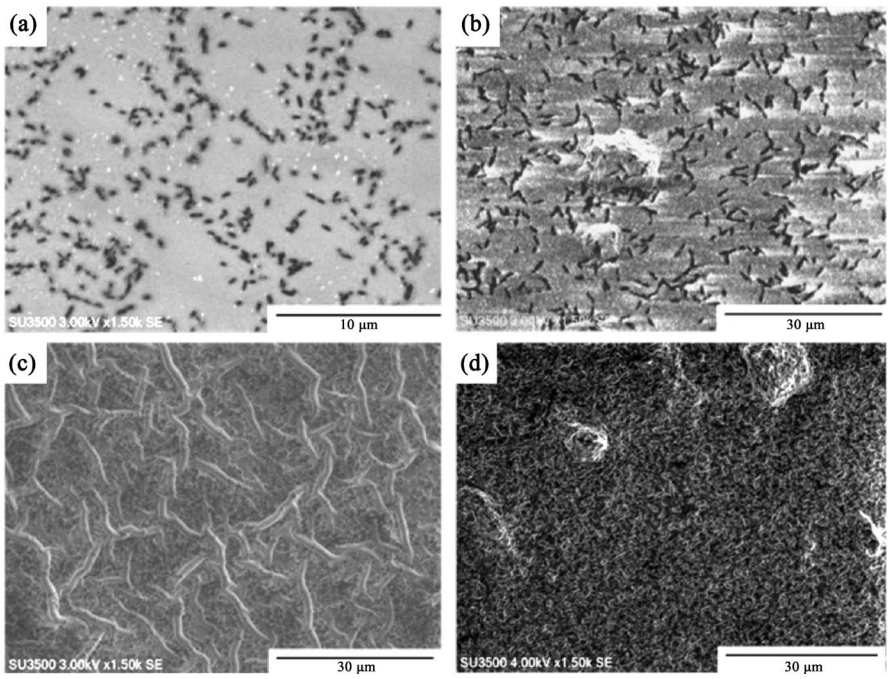

Figure 6. SEM images for *Shewanella oneidensis* MR-1 attached to (a) the bare ITO electrode, (b) the SYn-1/ITO electrode, (c) the SWy-1/ITO electrode, and (d) the NAu-1/ITO electrode.

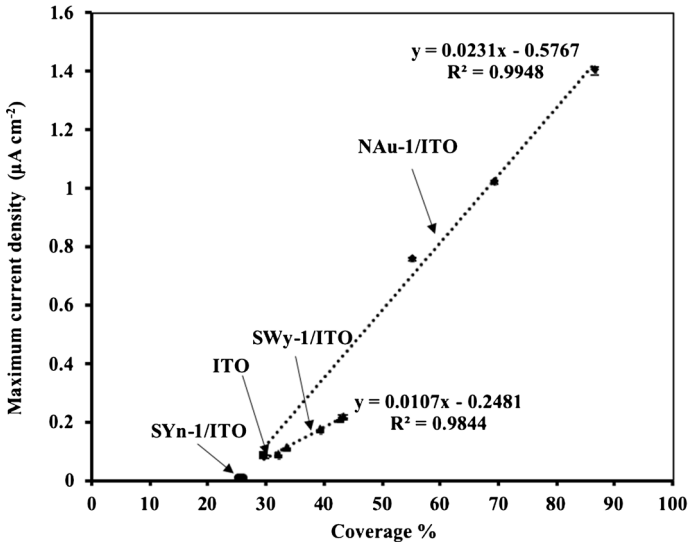

Figure 7. Maximum current densities obtained by *Shewanella oneidensis* MR-1 for different bacterial cell area coverage percentages on the clay-modified ITO electrodes.

maximum current density obtained by *Shewanella oneidensis* MR-1 and the area coverage percentage of bacterial cells on the clay-modified ITO electrodes. The area coverage for the bare ITO electrode (black square, ~30%) was used as a comparison.

As indicated by the differences in slopes of the two lines presented in **Figure 7**, the increase in the coverage percentage was higher for NAu-1/ITO than for SWy1/ITO. This can be accounted for by considering **Table 1**, since NAu-1 contains a greater quantity of iron than SWy-1, and so the number of Fe^{3+} ions available for electron transfer will be significantly greater in the case of the NAu-1/ITO electrode, thereby allowing for a larger bacterial surface coverage. In addition, we note that the iron-free SYn-1/ITO clay has a similar bacterial coverage percentage to that of the bare ITO, thereby indicating that the Fe^{3+} ions present in the clay not only promote the electron transfer process, but they also attract bacterial cells for attachment to the electrode. These findings indicate that there is a direct relationship between the obtained current density and the number of bacterial cells attached to the electrode, where greater numbers of bacteria result in higher currents.

4. Conclusion

We herein reported our investigation into the role of the structural iron present in clays in enhancing the electron transfer of *Shewanella oneidensis* MR-1. For this purpose, three types of clay containing different iron loadings were used to modify ITO (indium tin oxide) electrodes, namely nontronite NAu-1, montmorillonite (Wyoming) SWy-1, and synthetic montmorillonite SYn-1. The particle size, porosity, coverage, and film thickness of each clay were examined, and ferricyanide experiments confirmed that the desired clay-modified ITO electrodes were successfully prepared, where an increased electrode film thickness inhibited

diffusion of the ferricyanide anion, thereby suggesting a higher film coverage consistent with scanning electron microscopy measurements. Interestingly, the various clay-modified ITO electrodes gave different results upon combination with *Shewanella oneidensis* MR-1. More specifically, increasing the film thicknesses of the NAu-1/ITO and SWy-1/ITO clays resulted in increased current densities, reduction peak currents, and bacterial cell attachments, while in the case of SYn-1/ITO, increasing the film thickness had no effect on the above factors. This was attributed to the fact that NAu-1 and SWy-1 both contain iron, which transfers electrons to the ITO and promotes bacterial attachment. We therefore expect that the inexpensive and nonchemical-based electrode modification technique reported herein could represent a promising modification for the development of microbial fuel cells.

Acknowledgements

This research utilized a scanning electron microscope, which was funded by the NSF, Major Research Instrumentation (MRI) Program via Award No. 1726994.

Conflicts of Interest

The authors declare no conflicts of interest regarding the publication of this paper.

References

[1] Wu, W., Lesnik, K.L., Xu, S., Wang, L. and Liu, H. (2014) Impact of Tobramycin on the Performance of Microbial Fuel Cell. *Microbial Cell Factories*, **13**, 91. https://doi.org/10.1186/s12934-014-0091-6

[2] Abourached, C., English, M.J. and Liu, H. (2016) Wastewater Treatment by Microbial Fuel Cell (MFC) Prior Irrigation Water Reuse. *Journal of Cleaner Production*, **137**, 144-149. https://doi.org/10.1016/j.jclepro.2016.07.048

[3] Liu, H., Ramnarayanan, R. and Logan, B.E. (2004) Production of Electricity during Wastewater Treatment Using a Single Chamber Microbial Fuel Cell. *Environmental Science & Technology*, **38**, 2281-2285. https://doi.org/10.1021/es034923g

[4] Cecconet, D., Callegari, A. and Capodaglio, A. (2018) Bioelectrochemical Systems for Removal of Selected Metals and Perchlorate from Groundwater: A Review. *Energies*, **11**, 2643. https://doi.org/10.3390/en11102643

[5] Baron, D., LaBelle, E., Coursolle, D., Gralnick, J.A. and Bond, D.R. (2009) Electrochemical Measurement of Electron Transfer Kinetics by *Shewanella oneidensis* MR-1. *Journal of Biological Chemistry*, **284**, 28865-28873. https://doi.org/10.1074/jbc.M109.043455

[6] Liao, Z.-H., Sun, J.-Z., Sun, D.-Z., Si, R.-W. and Yong, Y.-C. (2015) Enhancement of Power Production with Tartaric Acid Doped Polyaniline Nanowire Network Modified Anode in Microbial Fuel Cells. *Bioresource Technology*, **192**, 831-834. https://doi.org/10.1016/j.biortech.2015.05.105

[7] Pant, D., Van Bogaert, G., Diels, L. and Vanbroekhoven, K. (2010) A Review of the Substrates Used in Microbial Fuel Cells (MFCs) for Sustainable Energy Production. *Bioresource Technology*, **101**, 1533-1543. https://doi.org/10.1016/j.biortech.2009.10.017

[8] Zhang, C., Zhang, D. and Xiao, Z. (2019) Application of Redox Mediators in Bioelectrochemical System. In: Wang, A.J., Liang, B., Li, Z.L. and Cheng, H.Y., Eds., *Bioelectrochemistry Stimulated Environmental Remediation*, Springer, Amsterdam, 205-226. https://doi.org/10.1007/978-981-10-8542-0_8

[9] Logan, B.E., Wallack, M.J., Kim, K.-Y., He, W., Feng, Y. and Saikaly, P.E. (2015) Assessment of Microbial Fuel Cell Configurations and Power Densities. *Environmental Science & Technology Letters*, **2**, 206-214. https://doi.org/10.1021/acs.estlett.5b00180

[10] Wu, W., Niu, H., Yang, D., Wang, S.-B., Wang, J., Lin, J. and Hu, C. (2019) Controlled Layer-By-Layer Deposition of Carbon Nanotubes on Electrodes for Microbial Fuel Cells. *Energies*, **12**, 363. https://doi.org/10.3390/en12030363

[11] Ji, J., Jia, Y., Wu, W., Bai, L., Ge, L. and Gu, Z. (2011) A Layer-by-Layer Self-Assembled Fe_2O_3 Nanorod-Based Composite Multilayer Film on ITO Anode in Microbial Fuel Cell. *Colloids and Surfaces A*: *Physicochemical and Engineering Aspects*, **390**, 56-61. https://doi.org/10.1016/j.colsurfa.2011.08.056

[12] Zhu, Y., Ji, J., Ren, J., Yao, C. and Ge, L. (2014) Conductive Multilayered Polyelectrolyte Films Improved Performance in Microbial Fuel Cells (MFCs). *Colloids and Surfaces A*: *Physicochemical and Engineering Aspects*, **455**, 92-96. https://doi.org/10.1016/j.colsurfa.2014.04.030

[13] Dong, H. (2012) Clay-Microbe Interactions and Implications for Environmental Mitigation. *Scientific Reports*, **7**, 113-118. https://doi.org/10.2113/gselements.8.2.113

[14] Beall, G.W. (2003) The Use of Organo-Clays in Water Treatment. *Applied Clay Science*, **24**, 11-20. https://doi.org/10.1016/j.clay.2003.07.006

[15] Fitch, A. (2002) Electrochemical Properties of Clays. The Clay Minerals Society, Chantilly, VA. https://doi.org/10.1346/CMS-WLS-10

[16] Fripiat, H.V.O. (2019) Source Clay Physical/Chemical Data. http://www.clays.org/sourceclays_data.html

[17] Koo, T.-H., Jang, Y.-N., Kogure, T., Kim, J.H., Park, B.C., Sunwoo, D. and Kim, J.-W. (2014) Structural and Chemical Modification of Nontronite Associated with Microbial Fe(III) Reduction: Indicators of "Illitization". *Chemical Geology*, **377**, 87-95. https://doi.org/10.1016/j.chemgeo.2014.04.005

[18] An, N., Zhou, C.H., Zhuang, X.Y., Tong, D.S. and Yu, W.H. (2015) Immobilization of Enzymes on Clay Minerals for Biocatalysts and Biosensors. *Applied Clay Science*, **114**, 283-296. https://doi.org/10.1016/j.clay.2015.05.029

[19] Unal, B., Yalcinkaya, E.E., Demirkol, D.O. and Timur, S. (2018) An Electrospun Nanofiber Matrix Based on Organo-Clay for Biosensors: PVA/PAMAM-Montmorillonite. *Applied Surface Science*, **444**, 542-551. https://doi.org/10.1016/j.apsusc.2018.03.109

[20] Mousty, C. (2004) Sensors and Biosensors Based on Clay-Modified Electrodes—New Trends. *Applied Clay Science*, **27**, 159-177. https://doi.org/10.1016/j.clay.2004.06.005

[21] Zen, J.-M. and Kumar, A.S. (2004) Peer Reviewed: The Prospects of Clay Mineral Electrodes. *Analytical Chemistry*, **76**, 205A-211A. https://doi.org/10.1021/ac041566z

[22] Yao, K., Shimazu, K., Nakata, M. and Yamagishi, A. (1998) Clay-Modified Electrodes as Studied by the Quartz Crystal Microbalance: Adsorption of Ruthenium Complexes. *Journal of Electroanalytical Chemistry*, **442**, 235-242. https://doi.org/10.1016/S0022-0728(97)00445-2

[23] Yao, K., Taniguchi, M., Nakata, M., Shimazu, K., Takahashi, M. and Yamagishi, A. (1998) Mass Transport on an Anionic Clay-Modified Electrode as Studied by a Quartz Crystal Microbalance. *Journal of Electroanalytical Chemistry*, **457**, 119-128. https://doi.org/10.1016/S0022-0728(98)00309-X

[24] Xiang, Y. and Villemure, G. (1992) Electron Transport in Clay-Modified Electrodes: Study of Electron Transfer between Electrochemically Oxidized Tris (2,2'-Bipyridyl) Iron Cations and Clay Structural Iron(II) Sites. *Canadian Journal of Chemistry*, **70**, 1833-1837. https://doi.org/10.1139/v92-227

[25] Xiang, Y. and Villemure, G. (1995) Electrodes Modified with Synthetic Clay Minerals: Evidence of Direct Electron Transfer from Structural Iron Sites in the Clay Lattice. *Journal of Electroanalytical Chemistry*, **381**, 21-27. https://doi.org/10.1016/0022-0728(94)03629-H

[26] Lei, C., Lisdat, F., Wollenberger, U. and Scheller, F.W. (1999) Cytochrome c/Clay-Modified Electrode. *Electroanalysis*: *An International Journal Devoted to Fundamental and Practical Aspects of Electroanalysis*, **11**, 274-276. https://doi.org/10.1002/(SICI)1521-4109(199904)11:4<274::AID-ELAN274>3.0.CO;2-G

[27] Charradi, K., Forano, C., Prevot, V., Ben Haj Amara, A. and Mousty, C. (2009) Direct Electron Transfer and Enhanced Electrocatalytic Activity of Hemoglobin at Iron-Rich Clay Modified Electrodes. *Langmuir*, **25**, 10376-10383. https://doi.org/10.1021/la901080r

[28] Charradi, K., Gondran, C., Amara, A.B.H., Prevot, V. and Mousty, C. (2009) H_2O_2 Determination at Iron-Rich Clay Modified Electrodes. *Electrochimica Acta*, **54**, 4237-4244. https://doi.org/10.1016/j.electacta.2009.02.078

[29] Koffi, O., Bile, B., Bengourram, J., Tankiouine, S. and Latrache, H. (2016) Electrochemical Study of Interaction of Bacteria and Clay. *Journal of Microbial and Biochemical Technology*, **8**, 60-64.

[30] Wu, W., Yang, F., Liu, X. and Bai, L. (2014) Influence of Substrate on Electricity Generation of *Shewanella loihica* PV-4 in Microbial Fuel Cells. *Microbial Cell Factories*, **13**, 69. https://doi.org/10.1186/1475-2859-13-69

[31] Tsai, W., Lai, C. and Hsien, K. (2003) Effect of Particle Size of Activated Clay on the Adsorption of Paraquat from Aqueous Solution. *Journal of Colloid and Interface Science*, **263**, 29-34. https://doi.org/10.1016/S0021-9797(03)00213-3

[32] Kozaki, T., Sato, Y., Nakajima, M., Kato, H., Sato, S. and Ohashi, H. (1999) Effect of Particle Size on the Diffusion Behavior of Some Radionuclides in Compacted Bentonite. *Journal of Nuclear Materials*, **270**, 265-272. https://doi.org/10.1016/S0022-3115(98)00782-X

[33] Qiao, Y., Li, C.M., Bao, S.-J. and Bao, Q.-L. (2007) Carbon Nanotube/Polyaniline Composite as Anode Material for Microbial Fuel Cells. *Journal of Power Sources*, **170**, 79-84. https://doi.org/10.1016/j.jpowsour.2007.03.048

[34] Stein, J.A. and Fitch, A. (1996) Effect of Clay Type on the Diffusional Properties of a Clay-Modified Electrode. *Clays and Clay Minerals*, **44**, 381-392.

[35] Fitch, A., Du, J., Gan, H. and Stucki, J.W. (1995) Effect of Clay Charge on Swelling: A Clay-Modified Electrode Study. *Clays and Clay Minerals*, **43**, 607-614.

[36] Macha, S., Zayia, G., Du, J., Stein, J. and Fitch, A. (1999) Diffusion Control in Thin Clay Films: Tailoring Layered Clay Film Structures through Control of Aqueous Electrolyte. *Applied Clay Science*, **15**, 153-172. https://doi.org/10.1016/S0169-1317(99)00022-8

[37] Kostka, J.E., Dalton, D.D., Skelton, H., Dollhopf, S. and Stucki, J.W. (2002) Growth of Iron(III)-Reducing Bacteria on Clay Minerals as the Sole Electron Acceptor and Comparison of Growth Yields on a Variety of Oxidized Iron Forms. *Applied Environmental Microbiology*, **68**, 6256-6262. https://doi.org/10.1128/AEM.68.12.6256-6262.2002

[38] Stucki, J.W., Komadel, P. and Wilkinson, H.T. (1987) Microbial Reduction of Structural Iron(III) in Smectites. *Soil Science Society of America Journal*, **51**, 1663-1665. https://doi.org/10.2136/sssaj1987.03615995005100060047x

[39] Kostka, J.E., Wu, J., Nealson, K.H. and Stucki, J.W. (1999) The Impact of Structural Fe (III) Reduction by Bacteria on the Surface Chemistry of Smectite Clay Minerals. *Geochimica et Cosmochimica Acta*, **63**, 3705-3713. https://doi.org/10.1016/S0016-7037(99)00199-4

[40] Dong, H., Kukkadapu, R.K., Fredrickson, J.K., Zachara, J.M., Kennedy, D.W. and Kostandarithes, H.M. (2003) Microbial Reduction of Structural Fe(III) in Illite and Goethite. *Environmental Science & Technology*, **37**, 1268-1276. https://doi.org/10.1021/es020919d

[41] Schaefer, M.V., Gorski, C.A. and Scherer, M.M. (2010) Spectroscopic Evidence for Interfacial Fe(II)-Fe(III) Electron Transfer in a Clay Mineral. *Environmental Science & Technology*, **45**, 540-545. https://doi.org/10.1021/es102560m

[42] Hofstetter, T.B., Neumann, A. and Schwarzenbach, R.P. (2006) Reduction of Nitroaromatic Compounds by Fe(II) Species Associated with Iron-Rich Smectites. *Environmental Science & Technology*, **40**, 235-242. https://doi.org/10.1021/es0515147

[43] Lee, W. and Batchelor, B. (2003) Reductive Capacity of Natural Reductants. *Environmental Science & Technology*, **37**, 535-541. https://doi.org/10.1021/es025830m

[44] Neumann, A., Hofstetter, T.B., Schwarzenbach, R.P. and Skarpeli-Liati, M. (2009) Reduction of Polychlorinated Ethanes and Carbon Tetrachloride by Structural Fe(II) in Smectites. *Environmental Science & Technology*, **43**, 4082-4089. https://doi.org/10.1021/es9001967

[45] Brigatti, M.F., Franchini, G., Lugli, C., Medici, L., Poppi, L. and Turci, E. (2000) Interaction between Aqueous Chromium Solutions and Layer Silicates. *Applied Geochemistry*, **15**, 1307-1316. https://doi.org/10.1016/S0883-2927(99)00120-1

[46] Ilton, E.S., Haiduc, A., Moses, C.O., Heald, S.M., Elbert, D.C. and Veblen, D.R. (2004) Heterogeneous Reduction of Uranyl by Micas: Crystal Chemical and Solution Controls. *Geochimica et Cosmochimica Acta*, **68**, 2417-2435. https://doi.org/10.1016/j.gca.2003.08.010

[47] Peretyazhko, T., Zachara, J.M., Heald, S.M., Jeon, B.-H., Kukkadapu, R.K., Liu, C., Moore, D. and Resch, C.T. (2008) Heterogeneous Reduction of Tc(VII) by Fe(II) at the Solid-Water Interface. *Geochimica et Cosmochimica Acta*, **72**, 1521-1539. https://doi.org/10.1016/j.gca.2008.01.004

[48] Lee, K., Kostka, J.E. and Stucki, J.W. (2006) Comparisons of Structural Fe Reduction in Smectites by Bacteria and Dithionite: An Infrared Spectroscopic Study. *Clays and Clay Minerals*, **54**, 195-208. https://doi.org/10.1346/CCMN.2006.0540205

[49] Ribeiro, F.R., Fabris, J.D., Kostka, J.E., Komadel, P., Stucki, J.W. (2009) Comparisons of Structural Iron Reduction in Smectites by Bacteria and Dithionite: II. A Variable-Temperature Mössbauer Spectroscopic Study of Garfield Nontronite. *Pure and Applied Chemistry*, **81**, 1499-1509. https://doi.org/10.1351/PAC-CON-08-11-16

[50] Neumann, A., Petit, S.B. and Hofstetter, T. (2011) Evaluation of Redox-Active Iron

Sites in Smectites Using Middle and Near Infrared Spectroscopy. *Geochimica et Cosmochimica Acta*, **75**, 2336-2355. https://doi.org/10.1016/j.gca.2011.02.009

[51] Claire, F., Huo, D., Yan, L., Wu, J. and Stucki, J. (2002) Infrared Study of Reduced and Reduced-Reoxidized Ferruginous Smectite. *Clays and Clay Minerals*, **50**, 455-469. https://doi.org/10.1346/000986002320514181

[52] Claire, F., Huo, D., Yan, L., Wu, J. and Stucki, J. (2002) Effect of Fe Oxidation State on the IR Spectra of Garfield Nontronite. *American Mineralogist*, **87**, 630-641. https://doi.org/10.2138/am-2002-5-605

[53] Yan, L. and Stucki, J. (1999) Effects of Structural Fe Oxidation State on the Coupling of Interlayer Water and Structural Si-O Stretching Vibrations in Montmorillonite. *Langmuir*, **15**, 4648-4657. https://doi.org/10.1021/la9809022

[54] Lower, S.K., Hochella Jr., M.F. and Beveridge, T.J. (2001) Bacterial Recognition of Mineral Surfaces: Nanoscale Interactions between Shewanella and α-FeOOH. *Science*, **292**, 1360-1363. https://doi.org/10.1126/science.1059567

[55] Lower, B.H., Shi, L., Yongsunthon, R., Droubay, T.C., McCready, D.E. and Lower, S.K. (2007) Specific Bonds between an Iron Oxide Surface and Outer Membrane Cytochromes MtrC and OmcA from *Shewanella oneidensis* MR-1. *Journal of Bacteriology*, **189**, 4944-4952. https://doi.org/10.1128/JB.01518-06

[56] Lower, B.H., Yongsunthon, R., Shi, L., Wildling, L., Gruber, H.J., Wigginton, N.S., Reardon, C.L., Pinchuk, G.E., Droubay, T.C., Boily, J.F. and Lower, S.K. (2009) Antibody Recognition Force Microscopy Shows that Outer Membrane Cytochromes OmcA and MtrC Are Expressed on the Exterior Surface of *Shewanella oneidensis* MR-1. *Applied Environmental Microbiology*, **75**, 2931-2935. https://doi.org/10.1128/AEM.02108-08

[57] Reardon, C.L., Dohnalkova, A.C., Nachimuthu, P., Kennedy, D.W., Saffarini, D.A., Arey, B.W., Shi, L., Wang, Z., Moore, D., McLean, J.S., Moyles, D., Marshall, M.J., Zachara, J.M., Fredrickson, J.K. and Beliaev, A.S. (2010) Role of Outer-Membrane Cytochromes MtrC and OmcA in the Biomineralization of Ferrihydrite by *Shewanella oneidensis* MR-1. *Geobiology*, **8**, 56-68. https://doi.org/10.1111/j.1472-4669.2009.00226.x

[58] Kim, B.H., Kim, H.J., Hyun, M.S. and Park, D.H. (1999) Direct Electrode Reaction of Fe(III)-Reducing Bacterium, *Shewanella putrefaciens*. *Journal of Microbiology and Biotechnology*, **9**, 127-131.

[59] Meitl, L.A., Eggleston, C.M., Colberg, P.J.S., Khare, N., Reardon, C.L. and Shi, L. (2009) Electrochemical Interaction of *Shewanella oneidensis* MR-1 and Its Outer Membrane Cytochromes OmcA and MtrC with Hematite Electrodes. *Geochimica et Cosmochimica Acta*, **73**, 5292-5307. https://doi.org/10.1016/j.gca.2009.06.021